

# PREDICTING STRAIN RATE DURING IR IMAGING OF TENSILE DEFORMATION USING MLP BASED ANN

B.Venkatraman, C.Rajagopalan and Baldev Raj

Materials Chemical and Reprocessing Group, Indira Gandhi Centre for Atomic Research  
Kalpakkam, India

**Abstract :** During tensile testing, a part of the mechanical work done on the specimen is transformed into heat energy. Using thermal imaging, it is possible to detect and measure the variation of temperature and relate it to the deformation behaviour of the material. It is now well established that Artificial Neural Networks(ANN) can be used to solve complex non-linear classification and prediction problems. In thermal NDE, ANNs have been used in a very limited way, mainly for defect analysis and classification. In this paper, we establish the feasibility of using multi-layered perceptron based ANN for predicting the strain rate during tensile deformation of nuclear grade Type 316 Stainless Steel with prediction errors less than 2.7%. This approach provides feasibility to interpolate and determine the stress or temperature based on minimum experiments and can also be applied to industrial components.

**Introduction :** It is well known that during tensile testing, a part of the mechanical work done on the specimen is transformed into heat energy. The maximum temperature and the rate of temperature rise is related to the nature of the material, test conditions and the deformation behaviour of the material during loading. Using infrared (IR) imaging, it is possible to detect the variations in temperature and consequently predict the deformation behaviour of the material. Thus, IR imaging can be viewed as an adjunct to conventional mechanical test techniques. Apart from the basic advantage of non contact measurement, the technique offers itself to the detection of transient exothermic or endothermic changes that cannot be normally observed through conventional testing practices. This kind of work, though initiated by Wilburn [1] and Y.Huang [2], is limited. In all the investigations pursued so far, experiments have been on measurement of temperature and relating it to the mechanical properties. At the authors' laboratory, for the first time both IR imaging and acoustic emission (AE) have been successfully used to characterise the various stages of tensile deformation of a nuclear grade AISI type 316 stainless steel (SS) [3,4]. Recent years have seen extensive applications of ANN to solve complex problems, particularly where the analytical relationship between the input and output values of a system are unknown. ANNs are powerful, robust and adaptive tools for detection and classification of features under changing signature or environmental conditions. They are also known for their processing speed, high classification accuracy, low-sensitivity to noise and flexible thresholding capability. These networks can be trained from a set of observed examples (called the training set) and then applied on other similar data not contained in the training set.

In the field of thermal NDE, the reported applications of ANN are only a few. ANNs have been primarily used for defect feature extraction and classification [5-12] and in one case for depth estimation [13]. The application of ANN for analysis of the thermal measurements obtained from tensile tests and the concept of predicting the temperature or stress, based on experimental interpolations has not been attempted so far. Such an approach provides opportunities to interpolate and determine the stress or temperature based on minimum experiments. In this paper, we explore the feasibility of this new idea of using multi-layered, error-back-propagating, feed-forward artificial neural network (MLP-ANN) for predicting the temperature and strain rate during tensile deformation of nuclear grade AISI Type 316 SS.

**General Architecture of the MLP :** The multilayered perceptron (MLP) is one of the most versatile artificial neural networks and is popular for data classification and prediction applications. The basic architecture of the MLP neural network is shown in Figure 1. The first layer, known as the input layer,

consists of a number of input nodes. In general, there will be one such node for each variable used to model the output. In this case, it corresponds to the IR parameter (feature) used for classification/ prediction. Let  $M$  represent the maximum number of variables (components per input vector) so that there would be  $i = 1 \dots M$  nodes in the input layer. Each input vector  $X_i$  then has  $k = 1 \dots m$  values associated with it. The network contains one or more hidden layers and each node in the hidden layer is connected to every node in the previous layer through a set of weighted links. Let  $j$  represent nodes in a hidden layer with  $j = 1 \dots P$  such hidden layer nodes. Then there would be  $M \times P$  such weights  $W_{ij}$  connecting the input node to the hidden layer nodes. MLPs can have more than one hidden layer also. Following the hidden layers, is the output layer, which may contain a node for every variable that is to be modelled. Again, weights are used to connect each output nodes to every node in the previous hidden layer. With  $N$  output nodes and one hidden layer, there will be  $N \times P$  such weights  $W_{jf}$  connecting the hidden layer nodes to the output nodes.

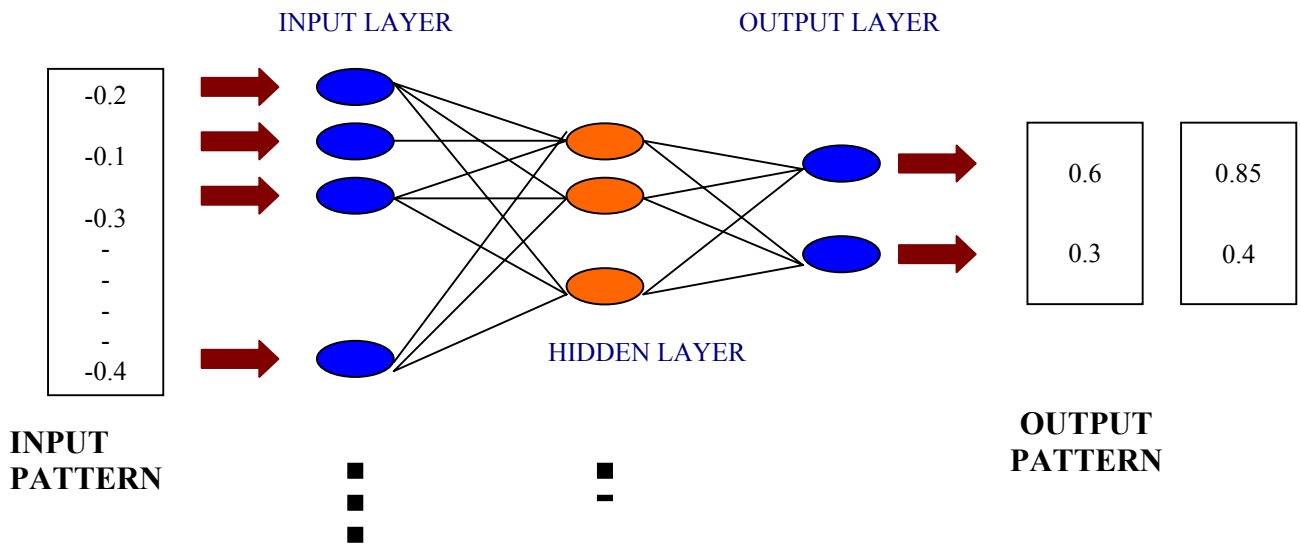


Figure 1. Basic Architecture of Multilayered Perceptron based

The MLP can be viewed as a network whose weights are used to map a series of input patterns (or feature vectors) into the required output. Final values of all the link weights are obtained by a training process carried out by passing a set of inputs (in our case these are strain, temperature, strain rate, cross head speed and stress) through the MLP and adjusting the weights to minimize the error between the result the network gives for output  $Y_{fk}^p$  and the actual output value  $Y_{fk}$ . This is repeated for all the input combinations and the final weights are those that minimize the average of all  $n$  squared errors. Once the weights have been set, the network is able to produce predictions for the output using input values not used during the training process.

Figure 2 shows the training process in more detail by illustrating the inputs between four input nodes ( $i = 1$  to 4) and a single node (node  $j$ ) in the hidden layer. A set of input values  $X_{1k}$  to  $X_{4k}$  (where  $X_{1k}$  to  $X_{4k}$  might be temperature / nominal strain/ stress obtained during tensile deformation - for example is presented to the network and a weighted sum of these values is formed using the relevant weights ( $W_{1j}$  to  $W_{4j}$ ). This weighted sum  $U_{jk}$  is then passed through a non-linear activation function  $f(U_{jk})$  to produce an output  $Y_{jk}$  in the range 0 to 1. It is because of this activation function that the MLP is ideal for modelling non-linear relationships such as that between temperature generated and strain or strain rate. This output is then sent to a node in the next hidden layer or to an output node where a similar weighting and normalization procedure takes place. The result will be an output prediction in the range 0 to 1. To allow comparison to be made, the output data must be rescaled in this range before analysis. It is also advisable to rescale all inputs into a similar range so that the weighted sums described above are often calculated on the scaled inputs.

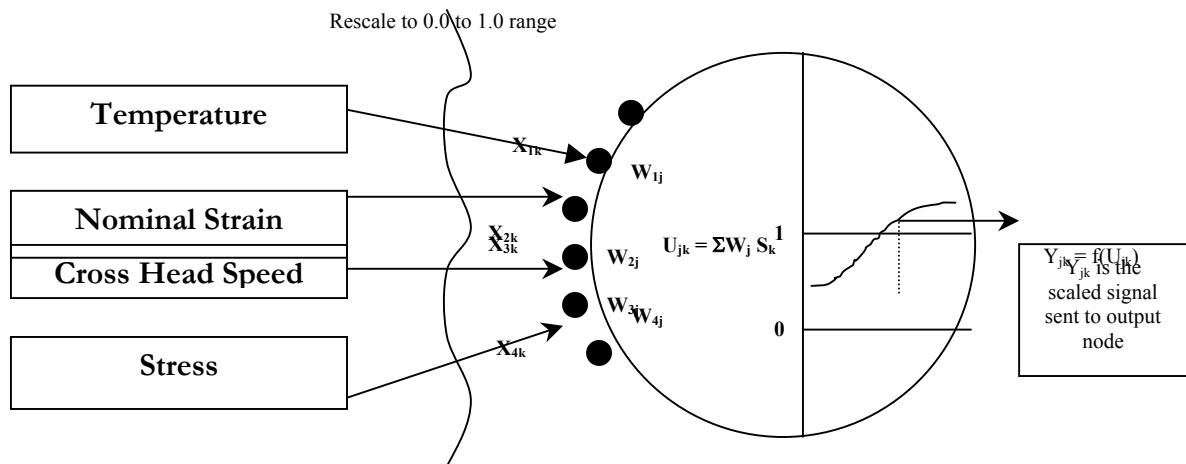


Figure 2. Feed forward procedure through a part of the network

**Use of MLP-ANN for Strain Rate Prediction :** The parameters used in this study are (a) stress, (b) nominal strain, (c) maximum temperatures and (d) strain rates corresponding to cross head velocity of 1 mm/min, 2 mm/min, 5 mm/min, 10 mm/min and 50 mm/min. The experimental data is obtained as follows. The stress and nominal strain values for a given strain rate are determined from the stress strain curves. The thermal images of the deformation process are acquired using the infrared imaging system Agema Thermovision 550. This system has a thermal resolution of 0.1 K at 303 K and a spatial resolution better than 1.1 mrad. The thermal values are corrected for emissivity variations and also distance effects. The maximum temperature along the gage length of the specimen is obtained by thermal profiling and using spot temperature measurement function. As mentioned above, experiments were conducted at five different strain rates namely  $3.3 \times 10^{-4}$ ,  $6.7 \times 10^{-4}$ ,  $1.7 \times 10^{-3}$ ,  $3.3 \times 10^{-3}$ ,  $6.7 \times 10^{-3}$ ,  $1.7 \times 10^{-2}$ . The minimum strain rate was  $3.3 \times 10^{-4} \text{ s}^{-1}$  while the maximum strain rate was  $1.7 \times 10^{-2} \text{ s}^{-1}$ . The MLP-ANN is trained to predict the strain rate, while feeding the other three parameters as inputs.

For the following neural network prediction study, the DESKPACK Software System (DSS) was used [14]. A total of 204 data vectors were used for predicting the strain rate values. The data vectors, being values from different physical quantities, were having wide ranging values. For example, the stress values and the temperatures were in hundreds, while the strain rates were fractional. In order to use these values in an

MLP-ANN effectively, these were mapped onto a scale between 0.1 and 0.9, so as to increase the efficiency of the MLP-ANN. While mapping these values, the scaling factors were saved, so that a reverse mapping could be done later to compare the original (strain rate) values with the predicted values.

Figure 3 shows the DSS dialog box for a typical case of such reversible mapping performed on these data vectors. Note that mapping can be done either in the forward direction (Original Value  $\rightarrow$  to range [0.1, 0.9]) or in the reverse direction (range [0.1, 0.9]  $\rightarrow$  Original Value); and it can be done either row wise or column wise. The 204 forward-mapped data vectors were divided into two sets (set1 and set2), each consisting of 102 vectors, using the DSS. After obtaining the two sets of input vectors viz., set1 and set2, in trial 1, the first set (set1) is used for training the MLP-ANN and the second set (set2) is used for testing (predicting). In trial 2, the second set (set2) is used for training the MLP-ANN and the first set (set1) is used for testing (predicting). Figure 4 shows the MLP-ANN of the DSS obtaining the input architecture for a typical training session.

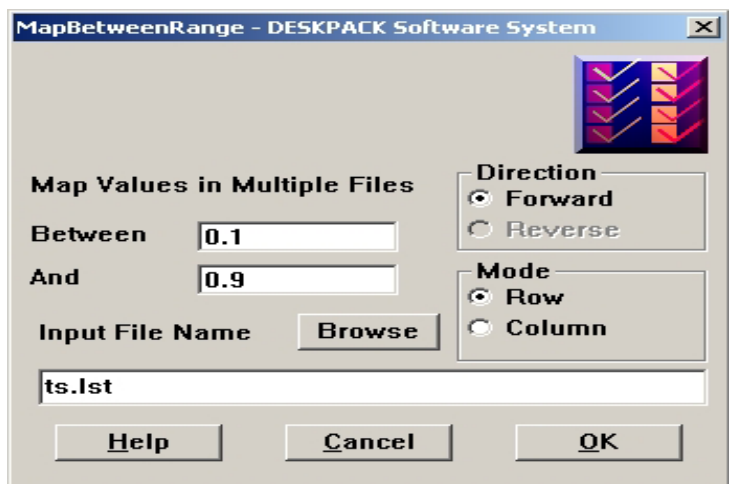


**Figure 3 DSS Dialog for reversible Mapping**

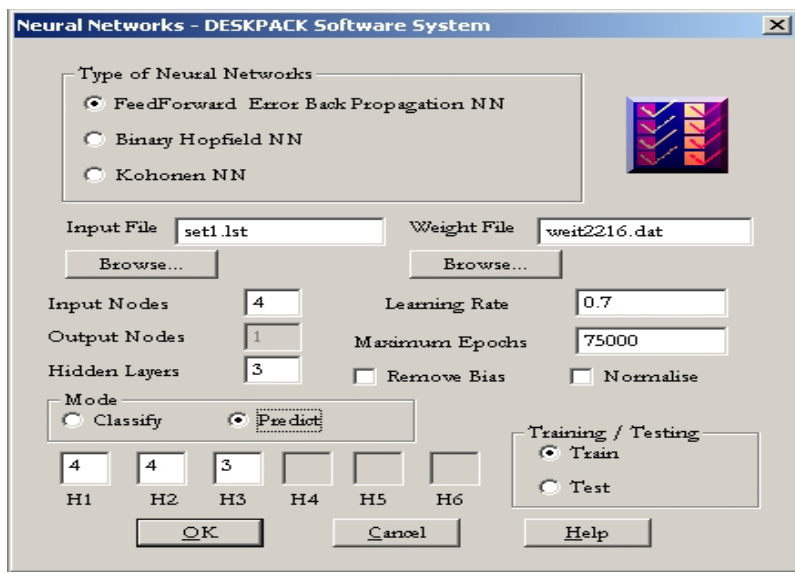


**Figure 4 MLP-ANN of the DSS obtaining the input architecture for a typical trial training session.**

For both trial 1 and trial 2, the MLP-ANN architecture used is 3-4-2-1. This architecture achieved the minimum pattern error in this study. The architectural details of this MLP-ANN are given in Table – 1.

**Table - 1 : Architectural Details of MLP – ANN**

Feature	Strain Rate Prediction
Input Nodes	3
Hidden Layer	3
Output Node	1 (for prediction)
Nodes in Hidden Layer 1	4
Nodes in Hidden Layer 2	3
Nodes in Hidden Layer 3	2
D.C.Bias Removal	No
Normalisation	No
Total Number of Files	102
Record Length of Each Signal	3
Mode (Train / Test)	Train
Learning Rate	0.500000 (Decreases with Epoch)
Completed Max Epochs...	150,000

Once the MLP-ANN was trained, a fresh set of 102 input feature vectors (each having three components, and normalised between 0.1-0.9) were used for testing the performance of the network. The predicted values were mapped back to the original physical scale for comparison with true strain rates. The typical trial oscillation of the pattern error and its subsequent reduction to a minimum value is graphically shown in Figure 5.

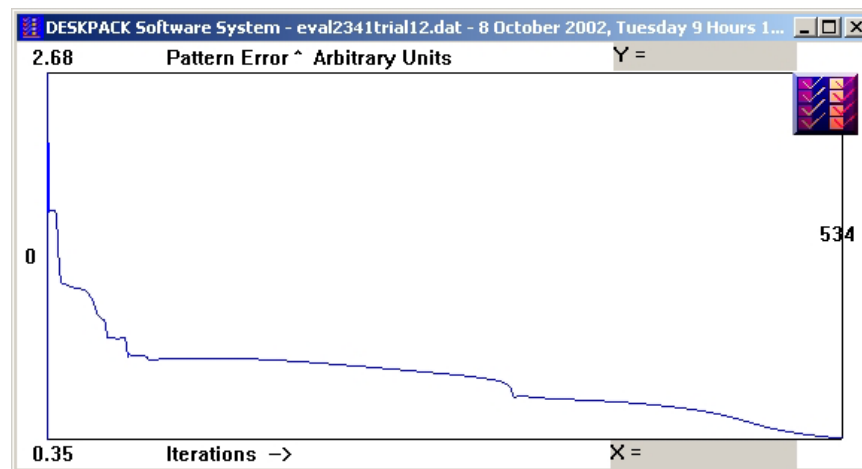


**Figure 5. Typical plot of the oscillation of the pattern error and its subsequent reduction to a minimum value**

**Results and Discussions :** The actual strain rate, predicted strain rate and the error in the predicted value is summarised in Table–3. It can be observed from the Table that the percentage error varies between – 2.72 % to 2.58 %. The reason for this is :

**Table – 3: True and Predicted Strain Rates**

<b>Strain rate Actual Value (s<sup>-1</sup>)</b>	<b>Strain rate Predicted value (s<sup>-1</sup>)</b>	<b>Error (%)</b>
0.00033	0.000319	-2.72
0.00067	0.000675	0.75
0.00330	0.003385	2.58
0.00670	0.006789	1.33
0.01700	0.016764	-1.39

(a) The strain rate varies two to three orders of magnitude spanning a wide range from  $10^{-4} \text{ s}^{-1}$  to  $10^{-2} \text{ s}^{-1}$ . For a single MLP-ANN (having fixed architecture and connecting weights), it would be rather difficult to predict the strain rate values that vary considerably.

(b) In addition, the number of input features that were used for the training of strain rate was minimal. However, in spite of these constraints, it can be observed that the MLP-ANN that was trained and tested, could still predict the strain rate with a good accuracy.

**Conclusion :** This study clearly establishes the feasibility of using this new idea of MLP-ANN for predicting the strain rate during tensile deformation of nuclear grade AISI type 316 SS. The overall error in the prediction of strain rate varies from about  $-2.72\%$  to  $-2.58\%$ . The reasons for this slightly larger error is attributed to the wide variations in the strain rate considered and also the minimal number of datasets used for training. The percentage errors can be further minimised by (a) Having more number of samples for training the network and (b) training the network to predict the strain rate only in a certain range and not covering all orders of magnitude – this should improve the accuracy of prediction considerably. Three areas of application that can be envisaged are

1. With minimum number of tensile tests it should be possible to interpolate and predict the temperatures or stress for any strain rate or vice versa based on ANN.
2. While in many cases heating due to inelastic deformation is of little consequence since the temperature rises are small, there are many important deformation processes where the rise in temperature is large enough to affect the mechanical / deformation properties. A typical example of such process is sheet metal forming. Using ANN based approach; it should be possible to predict the temperature under different heat transfer conditions. This would thus be very helpful to estimate the effects of differential temperature on materials and microstructures during such processes.
3. In many of the industrial components where the levels of stresses are known mapping the temperature profiles, it should be possible to predict the strain rate and thus the deformation behaviour of the material.

**Acknowledgements :** Authors are thankful to Shri P.Kalyanasundaram, Head, Division for PIE & NDT Development, IGCAR and Dr. T.Jayakumar, Head, NDT&E Section, DPEND, IGCAR for their valuable discussions. Authors are thankful to Dr.C.K.Mukhopadhyay for his experimental support.

**References :** 1.D.Wilburn, Temperature profiles observed in tensile specimens during physical test, Material Evaluation, March 1977, pp. 28-31.

2. Y.Huang, J.Xu, and C.H.Shih, Application of infrared technique to research on tensile test, *Material Evaluation*, December 1980, pp.76-79.
3. B.Venkataraman, Baldev Raj, C.K.Mukhopdhyay, and T.Jayakumar, Correlation of infrared thermographic patterns and acoustic emission signals with tensile deformation and fracture processes, In: D.O.Thompson, D.E.Chimenti, Editors, *Review of Progress in Quantitative NDE*, Vol. 20, USA, 2000, pp. 1443–50.
4. B.Venkataraman, Baldev Raj, and C.K.Mukhopdhyay, Characterisation of tensile deformation through infrared imaging technique, *Journal of the Korean Society for NDT*, Vol. 22, No. 6, 2002, pp. 609-620.
5. D.R.Prabhu, P.A.Howell, H.I.Syed, and W.P.Winfrey, Application of artificial neural networks to thermal detection of disbands, In: D.O.Thompson, D.E.Chimenti, Editors, *Review of Progress in Quantitative NDE*, Vol. 11B. New York: Plenum Press, 1992, pp. 1331-8.
6. D.R.Prabhu, and W.P.Winfrey, Neural network based processing of thermal NDE data for corrosion detection. *Ibid*, Vol. 12, 1993, pp. 478-86.
7. H.Tretout, D.David, J.Y.Marin, and M.Dessendre, An evaluation of artificial neural networks applied to infrared thermography inspection of composite aerospace structures. *Ibid*, Vol. 14. New York: Plenum Press, 1995, pp. 827-34.
8. P.G.Bison, C.Bressan, R.D.Sarno, E.Grinzato, S.Marinetti, and G.Manduchi, Thermal NDE of delaminations in plastics by neural network processing. In: D.Balageas, G.Busse, G.M.Carlomagno, Editors. *Proc. of Quantitative Infrared Thermography, Sorrento, Italy (QIRT 94, Eurotherm Seminar 42, Ed. Eur. Thermique et Industrie)*, 1994, pp. 214-19.
9. M.B.Santey, and D.P.Almond, An artificial neural network interpreter for transient thermography image data, *NDT&E International*, Vol. 30, No. 5, 1997, pp. 291-5.
10. Y.Largouet, A.Darabi, and X.Maldague, Depth evaluation in pulsed phase thermography with neural network. In: Thompson DO, Chimenti DE, editors. *Review of Progress in Quantitative NDE*, Vol. 18A. New York: Plenum Press, 1999, pp.611-17.
11. S.Vallerand, and X.Maldague, Defect characterization in pulsed thermography: a statistical method compared with Kohonen and perceptron neural networks. *NDT&E International*, Vol. 33, 2000, pp. 307-15.
12. E.Grinzato, S.Marinetti, P.G.Bison, and G.Manduchi, Application of neural networks to thermographic data reduction for non-destructive evaluation. *Revue Generale de Thermique* 1995, 34(397), pp. 17-27.
13. A.Darabi, and X.Maldague, Neural network based defect detection and depth estimation in TNDE. *NDT&E International*, Vol. 35, 2002, pp. 165-75.
14. C.Rajagopalan, *A Generic Knowledge-Based Systems' Architecture for Materials Evaluation*. Ph.D. Thesis, University of Madras, Chennai, 2000.